Melting of Olivine $(Mg, Fe)_2SiO_4$ Under High Pressure

Helen Nguyen

Advisor

Dr. Andrew Campbell
University of Maryland, College Park

Senior Thesis
Geology 394

November 21, 2007

Table of Contents

1. Abstract

Magnesium silicate perovskite (Pv) and magnesiowüstite (Mw) are the two most abundant minerals in the lower mantle. The purpose of my experiments is to observe the behaviors of Pv and Mw during partial melting in the lower mantle, and to understand which phase goes into the melt completely. My research is intended to resolve a discrepancy between two published papers. Campbell et al. (1992) concluded that the Pv phase appears to be the liquidus phase in the lower mantle at pressure between 30-40 GPa. Williams (1990) concluded that Mw appears to be the liquidus phase in the lower mantle, at pressures above 50 GPa. Ohtani et al. (1998) also report Mw on the liquidus at 25 GPa. My hypothesis is when melting of forsterite under lower mantle conditions; the liquidus phase is silicate Pv at 30-60 GPa.

2. Introduction

Partial melting of mantle material in the Earth's interior is one of the essential processes responsible for thermal and chemical evolution of the Earth. Mantle rock shallower than about 400 km depth consists mostly of olivine, pyroxenes, spinel and garnet; the typical rock type is peridotite (olivine-rich). Hypothetical primitive, undifferentiated mantle is called 'pyrolite' and is approximately 3 parts peridotite plus 1 part basalt. Between 400 km and 650 km depth, olivine is not stable and is replaced by high pressure polymorphs. Below 650 km, all of the minerals of the upper mantle begin to become unstable; the most abundant minerals present have the structure, but not the composition, of perovskite. The changes in mineralogy at about 400 to 650 km yield distinctive signatures in seismic records of the Earth's interior, and like the moho, are detected by using seismic waves.

The major minerals of the Earth's lower mantle are though to be $(Mg_{0.94}Fe_{0.06})SiO_3$ perovskite and magnesiowüstite $(Mg_{0.84}Fe_{0.16})O$ (Holland et el, 1997). The melting behavior of these assemblages is important for determining the temperature of the mantle and the origin of the seismically-imaged structures at the core-mantle boundary. Transformations in the Earth materials induced by pressure, as well as the combined effects of pressure and temperature, are the key to interpreting the composition of the lower mantle.

The interpretation and understanding of the geochemical differentiation of the Earth, geodynamics, rheology, and seismic tomography data hinge upon the melting temperatures of the lower mantle constituents. For example, differentiation strongly depends on the evolution of Earth's history, viscosity and anelasticity scaled with the ratio of actual temperature over melting temperature, and the melting temperature limits lateral temperature variations and the temperature contrast between the bottom of the mantle and the core.

3. Objectives of the Research

Previous work has been done in similar research, and the conclusions are different. Campbell et al. (1992) concluded that perovskite $(Mg,Fe)SiO_3$ is the liquidus phase, when melting olivine at lower mantle pressure between 30 to 40 GPa. Williams (1990) concluded that magnesiowüstite (Mg,Fe)O is the liquidus phase at lower mantle pressure above 50 GPa. Both studies used the laser-heated diamond anvil cell to generate high pressures and high temperatures in the laboratory.

In Campbell's experimental design, the samples were scanned under the laser beam at a rate of about 10 μm/sec forming a single stripe of heated material. The stripe ranged from 50 to 200 μm in length. The mineralogy of the recovered sample was studied by electron microscopy. The result was the silicate perovskite was found to be the liquidus phase in an assemblage of olivine composition at the lower mantle pressure. Iron, calcium, and manganese are found to behave as incompatible elements with respect to the Mg_2SiO_4 β- phase. Calcium partitioned more strongly, and manganese slightly less, than iron into the melt (Campbell et al., 1992).

In Williams's experimental design, his samples were scanned by a laser beam back and forth repeatedly, over the entire sample. He used infrared spectroscopy to study the recovered sample, including unmelted material near the surface of the sample, where it remained cold due to the highly conductive diamond anvils. Williams (1990) concluded from his laser-heated diamond cell studies that magnesiowüstite coexists with a silicate-rich liquid in systems of olivine composition above 50 GPa.

The melting temperature of Mg-Fe-Si-perovskite represents an upper bound for the melting temperature of the lower mantle (Zerr et al 1993). A more stringent upper bound would be the eutectic in the $(Mg,Fe)SiO_3$-(Mg,Fe)O system. The hypothesis I wish to test is that during melting of forsterite under lower mantle condition, the liquidus phase is silicate perovskite at 30 to 60 GPa.

4. Experimental Design

In order to obtain new constraints on the properties of an olivine-rich mantle at high pressures and temperatures, I used diamond anvil cells to carry out experiments at 30 to 60 GPa with single crystals of our starting material of olivine $(Mg_{0.9}Fe_{0.1}Ca_{0.001}Mn_{0.001})_2SiO_4$ surrounded by a NaCl or KBr pressure medium enclosed in steel gasket.

4.1 Property of Diamond

The principal components of a diamond cell are two diamond anvils compressing a gasket. A hole drilled in the center of the gasket serves as the pressure chamber. Diamond possesses not only very high strength, but also very high thermal conductivity, about 5 times that of copper (Boehler, 2000). The disadvantage of this property is that at high pressure a large portion of the heat produced in the sample by the laser is conducted away through the diamond anvils. This produces large temperature gradients in the laser-heated spot.

4.2 Polishing the Sample

I start out gluing a single crystal of olivine onto the glass slide with crystal bond. Using the 250 to 600 grit sand paper, I polished the sample until there is a flat and smooth surface on one side of the crystal. Then I put the glass slide on a hotplate to melt the crystal bond, and flipped the crystal to the other side, and continued polishing until it reach a smooth surface, and until the sample is thin enough for laser heating (ideally 10 μm or less). The sample was cleaned with acetone, which dissolves CrystalBond.

4.3 Loading the Sample

Loading the sample is the most difficult part of the experimental task, because of the microscopic nature of the starting materials. Also, they have to be carefully loaded and perfectly aligned between the diamond anvils to avoid damage to the diamonds during laser heating.

I started out with a 200 μm thick steel gasket, using the two aligned diamond culets size 300 μm across. I pre-indented the gasket down to a thickness of approximately 40 μm, and drilled a 90 μm hole in the center of the pre-indented area. A sample of olivine (<10 μm thick) is placed between KBr layers. KBr is used as an insulator to reduce the axial temperature gradient in the sample. The advantage of KBr is that it has a higher melting point than NaCl; otherwise it behaves the same as an insulator. Figure 1 illustrates the sample being loaded into the sample chamber between the KBr layers, with fine-grained rubies on top for pressure calibration.

4.4 Measuring the Pressure

The requirements for the pressure medium for laser heating experiments are (1) low shear strength, to minimize deviatoric stresses in the sample, (2) low thermal conductivity, in order to minimize laser focusing, (3) chemical inertness, (4) low absorption of the laser light, and (5) low emissivity, such that its emitted incandescent light is negligible in the measurement of the sample temperature (Boehler, 2000). NaCl and KBr meet all of these requirements. The disadvantage of these materials is their high

compressibility, which at high pressures reduces the thickness of the thermally insulating layer between the sample and the diamond.

Pressures in diamond anvil cells are measured routinely by the ruby fluorescence method (Mao et al, 1978). The method exploits the pressure dependence of the ruby fluorescence line, which can be excited by a blue or green laser. This pressure dependence has been calibrated by Mao et al. (1978). The standard deviation of these measurements is an estimate of uncertainty on pressure. My standard deviation on one of my sample is 0.5 GPa.

Pressure is raised by hand, using two allen wrenches to tighten the screws that drive the anvils toward each another. A green laser with 532 nm radiations is used to measure pressure, by measuring the wavelength of ruby fluorescence from ruby grains placed on top of the sample. Figure 2 illustrates the ruby fluorescence spectrum at 30 GPa. For each sample, I measured a variety of ruby grains across the sample chamber, and take the average of those measurements to get an accurate pressure measurement, because the pressure can be different from the rim to the core. The standard deviation of these measurements is an estimate of uncertainty on pressure.

4.5 Laser Heating

After compression, an infrared laser with 1.064 μm radiation is used to heat the sample held fixed under the beam, creating a laser-heated spot, the spot size is 30 μm. The diameter of the laser beam can be adjusted with the focusing optics and varied from 20 to 40 μm in these experiments.

One experimental difficulty was that the phase changes in the sample were accompanied by strong changes in laser light absorption. Olivine did not absorb the laser well, but its high P,T phases did. At first the sample did not absorb the laser very well; then there was a runaway effect during the laser heating, melting olivine at a very high peak temperature of 5200 K. Then we started out of making perovskite first giving us a controllable laser heating, when the perovskite was made then we started to melt the sample.

During the process of laser heating, we begun with a low laser power, slowly raised the laser power by 2% waiting a minute or two, until the sample suddenly becomes very hot, then shut off the laser power abruptly after two to five seconds of the heating, and the sample is cooled down to room temperature. Local equilibrium was obtained very rapidly during laser heating, because of the very high temperatures and small sample sizes, and the sample is quenched very quickly (~1ms).

At the very end of the research, we experimented with a new method to make the laser heating of olivine easier for future research. This was to add a small piece of platinum foil underneath the olivine to give us a jump start to help the olivine to absorb the laser power, and it helps to keep the melting temperature at around 3000 K.

4.6 Temperature Measurement

Temperature is determined by fitting the Planck radiation equation to the thermal emission of the sample. The Planck radiation function is used to calculate the temperature (T), from the measured intensities (I), at each wavelength (λ). C_1 and C_2 are constants, and ε is the emissivity.

$$I(\lambda) = \frac{\varepsilon c_1 \lambda^{-5}}{e^{c_2/\lambda T} - 1}$$

Figure 3 illustrate a laser heated spot. From the rim to the core, there is a change in temperature gradient indicate melting, and change in composition.

Two-dimensional temperature mapping of laser-heated diamond anvil cell samples is performed by processing a set of four simultaneous images of the sample, each obtained at a narrow spectral range in the visible to near-infrared (Campbell, 2007). The images are correlated spatially, and each set of four points is fit to the Planck radiation function to determine the temperature and the emissivity of the sample, using the gray body approximation. The advantages of this method is to measure the temperature and emissivity of the sample are mapped in two dimensions, chromatic aberrations are practically eliminated by independent focusing of each spectral band; and, all of the spectral images are obtained simultaneously, allowing temporal variations to be studied. As discussed by Campbell (2007), the accuracy of this method is approximately ±2%.

4.7 Recovering the Sample

After heating the sample, I decompressed the diamond-anvil cell, removed the gasket from the diamond tip, and carefully added tiny drops of water onto the sample to remove the KBr. The sample falls down onto a glass slide after the KBr is dissolved, and I mounted the sample on carbon tape. The sample and the carbon tape were mounted onto the glass slide, and then carefully carrying the sample right side up to the electron microprobe lab to have the composition examination.

4.8 Electron Microprobe Analysis

Before the products can be analyzed by the electron microprobe, they must be carbon coated. During the electron microprobe examination, I took measurements along a line running across the diameter of the laser-heated spots. With the assistance from Dr. Phil Piccoli and graduate student Noah Miller I obtained the images and the EDS analyses for my sample.

During the electron microprobe examination, I took measurements along a transect running across the diameter of the laser-heated spots. Because of the temperature gradient, the melt is concentrated in the center, and the solid phase on the liquidus forms a ring around the melted spot as illustrated in Figure 3. The main

observation to be made was whether this solid phase is silica-rich (perovskite) or silica-poor (magnesiowüstite), compared to the starting composition (olivine).

EDS analysis is better for this type of sample instead of using the WDS because this method is less sensitive to variations in topography, which is very important in these small and thin samples.

5. Results and Discussion

5.1 Results

Throughout the whole research I have made the total of fifteen samples. Ten samples were laser heated, two samples were not successfully heated because olivine did not absorbed the laser power very well, and the other three did not get heated because they were not loaded properly. Five laser-heated samples were successfully recovered; two samples successfully survived being repolished after the laser heating; four samples were being brought to the EMP to have analysis; and only two samples successfully produced EMP data. The table below showed a data summary of the samples.

Sample	Pressure	Standard Deviation	Temperature	EMP data obtained
HN1	30.06	0.33	1850 K*	No
HN2	30.71	0.10	2800 K*	Yes
HN3	30.78	0.15	3530 K*	No
HN4	30.64	0.15	1680 K*	No
HN5	40.26	0.21	3620 K*	Yes
HN7	40.69	0.18	5260 K	No
HN8	30.26	0.13	5240 K	No
HN10	40.03	0.11	2460 K	No

*An average temperature over the laser heated spot.

Sample HN1 was at 30 GPa, the average temperature that we found over the laser heated spot was 1850 K. This sample was filled with ruby, and with a low temperature that was measured we did not analysis in the EMP, and at this temperature we know that there is no melting.

Sample HN2 was at 30 GPa, the average temperature that we found over the laser heated spot was 2800 K. Figure 4 showed an SEM image that was taken from the EMP, we ran a 79.2 μm, 159 steps transect across the sample for and measured the composition, because of the temperature gradient, the melt is concentrated in the center, and the solid phase on the liquidus forms a ring around the melted spot. When we measured this sample in the EMP, the data showed no compositional changes across the heat sport, indicating that it probably did not melt.

Sample HN3, HN4 were at 30 GPa. The average temperature for HN3 is 3530 K, and HN4 is 1680 K. These two samples did not survive the recovery, therefore we have no EMP data of knowing if they were melted or how their phases changes.

Sample HN5 was at 40 GPa, the average temperature for this sample was 3620 K. Figure 5 showed an SEM image that was taken from EMP when obtaining the EDS data. Figure 6 showed the EDS data that we obtain from the electron microprobe for experiment at 40 GPa. We have the starting material to begin with, as coming into the rim of the sample we found that is MgO rich, and Si-poor. As going into the lighter part where there is Soret diffusion causes the variation with the melted region, where we saw Si-rich, and in the center is Fe-rich. From the EDM data, it indicated that the phase on the liquidus at 40 GPa is magnesiowüstite, not silicate perovskite.

Using the new temperature system, we could measure the temperature distribution throughout the laser heated spot. Sample HN8 was at 30 GPa, we found that the temperature is high above the published temperature of the pervoskite at the liquidus, we measured the temperature at 5240 K (Figure 7). Figure 8a and 8b showed the sample before and after heating.

Sample HN10, we measured the temperature at 40 GPa was at 2700 K. For this sample we added platinum in our sample chamber to absorb the laser better and reduce the runaway heating, so that the sample is melting at reasonable temperature. Figure 9 showed a 2-D temperature map across the laser heating spot. It was hard to recover this sample since it was embedded with the platinum foil; therefore I lost the sample while trying to polish it with the platinum foil.

5.2 Discussion

The temperature of the sample is sometimes a lot hotter (5200 K) in the center than is necessary to melt the sample. There are two factors affecting the compositional changes in the laser heated spots. First the outer rim of the laser heated spot is solid where the temperature is low (2000 K), at this temperature there is no melting occur. Where the solid meets the melt, the solid phase is the liquidus phase for the composition of our sample at high P,T. In the center of the laser heated spot its liquid where the temperature was high that indicated that there was melting occurred, and because the temperature is so high above the liquidus we saw chemical variations in the melted region were probably caused by Soret diffusion.

Soret diffusion is a process by which components tends to separate in a strong chemical gradient. If a temperature difference is applied between the boundaries of the mixture, as in my experiments, a composition gradient will appear at the steady state. In some of my samples (e.g. Figure 6) Soret diffusion clearly occurred in the central, melted region.

Sample HN5 was at 40 GPa, because we see a Fe-rich peak for the Fe/Mg+Fe ratio, we are uncertain if whether or not is Si-poor, due to the fact that the electron probe

only analysis at the very top surface of the laser heated spot, where we only see Fe-rich. There is a mass balance problem here; our EDS data shows a large Si-rich region, but not enough corresponding Si-poor region. There must be a Si-poor region in the center of the sample, deeper than our electron beam probed. This is why I re-polished that sample. To resolve this problem, we have polished the recovered product down further, then bring back the microprobe to re-analysis the inside portion of the laser heated spot. Unfortunately the sample broke during this handling, complicating the re-analysis. Nevertheless, the available EDS data showed that the magnesiowüstite appeared to be in the liquidus, not the silicate perovskite for experiment at 40 GPa.

6. Conclusion

The high pressures melting of lower mantle material are important for a number of geophysical and geochemical problems such as chemical differentiation and partial melting during the early evolution of the Earth. To be able to understand all of these, I loaded polished, single crystal olivine in a diamond anvil cell, pressure determined by measuring the wavelength of ruby fluorescence, temperature determined by fitting the Planck radiation equation to the thermal emission of the sample, composition measured by using the electron probe scanning linearly through the melting spot. The melt is concentrated in the center (hotspot) of the laser heated spot, and the coexisting solid forms a ring around the melt.

In conclusion, I would conclude that the EMP data indicate that the phase on the liquidus at 40 GPa is magnesiowüstite, not silicate perovskite.

Reference

Boehler, R. High-Pressure Experiments and the Phase Diagram of Lower Mantle and Core Materials. Geophysics, vol. 38. May, 2000.

Bina, Craig R.; Silver, Paul G. Constraints on lower mantle composition and temperature from density and bulk sound velocity profiles. Geophysical Research Letters, Volume 17, Issue 8, p. 1153-1156.

Campbell A. J. (2007) Measurement of temperature distributions across laser-heated samples by multispectral imaging radiometry. Submitted to *Rev. Sci. Instrum*.

Campbell A. J., Heinz D. L., and Davis A. M. (1992) Material transport in laser-heated diamond anvil cell melting experiments. *Geophys. Res. Lett.* 19, 1061-1064.

Hemley R J., Mao H.K. and Gramsch S.A. Pressure-induced transformations in deep mantle and core minerals. Mineralogical Magazine, April 2000, Vol. 64(2), pp. 157–184.

Holland, Kathleen G.; Thomas J. Ahrens. Melting of $(Mg,Fe)SiO_4$ at the Core-Mantle Boundary of the Earth. Science 14. March 1997.

Ohtani E., Moriwaki K., Kato T., and Onuma K. (1998) Melting and crystal-liquid partitioning in the system Mg2SiO4-Fe2SiO4 to 25 GPa. Phys. Earth Planet. Int. 107, 75-82.

Serghiou G., Zerr A., Boehler R. (Mg,Fe)SiO3-Perovskite Stability Under Lower Mantle Conditions. Science Vol. 280. June 1998, pp. 2093 – 2095.

Takahashi, E.; Ito, E. Melting of peridotite under very high pressure-II: A laboratory simulation for early evolution of the earth. NIPR, Tokyo, 8-10 June 1987, p. 77-79 (1987).

Watt, J. Peter; Ahrens, Thomas J. The role of iron partitioning in mantle composition, evolution, and scale of convection. Journal of Geophysical Research, Volume 87, Issue B7, p. 5631-5646.

Williams, Q. Molten $(Mg0.88Fe0.12)2SiO_4$ at lower mantle conditions – and structure of quenched glasses. Geophysical Research Letters, vol. 17, April 1990, p. 635-638.

Zerr, A.; Boehler, R. Melting of $(Mg,Fe)SiO_3$-Perovskite to 625 Kilobars: Indication of a High Melting Temperature in the Lower Mantle. Science, Volume 262, October 1993. p.553-555.

Figures

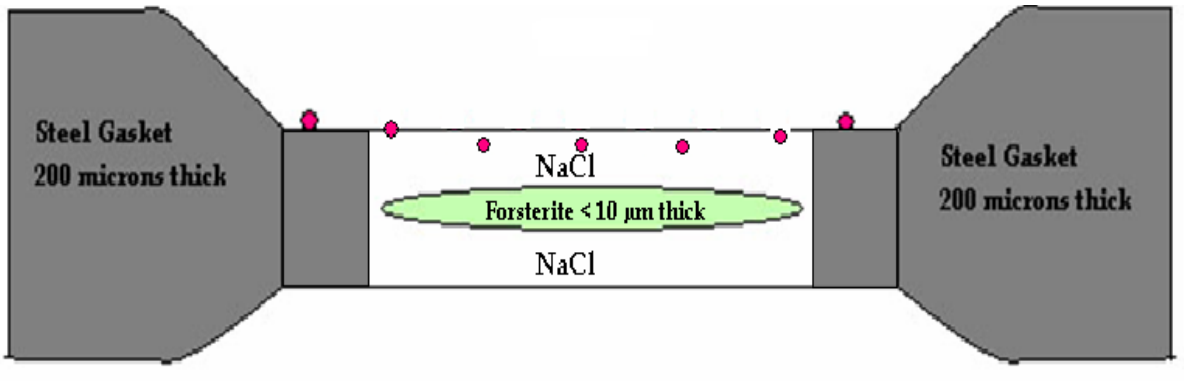

Figure 1. Starting composition $(Mg_{0.9}Fe_{0.1}Ca_{0.001}Mn_{0.001})_2SiO_4$

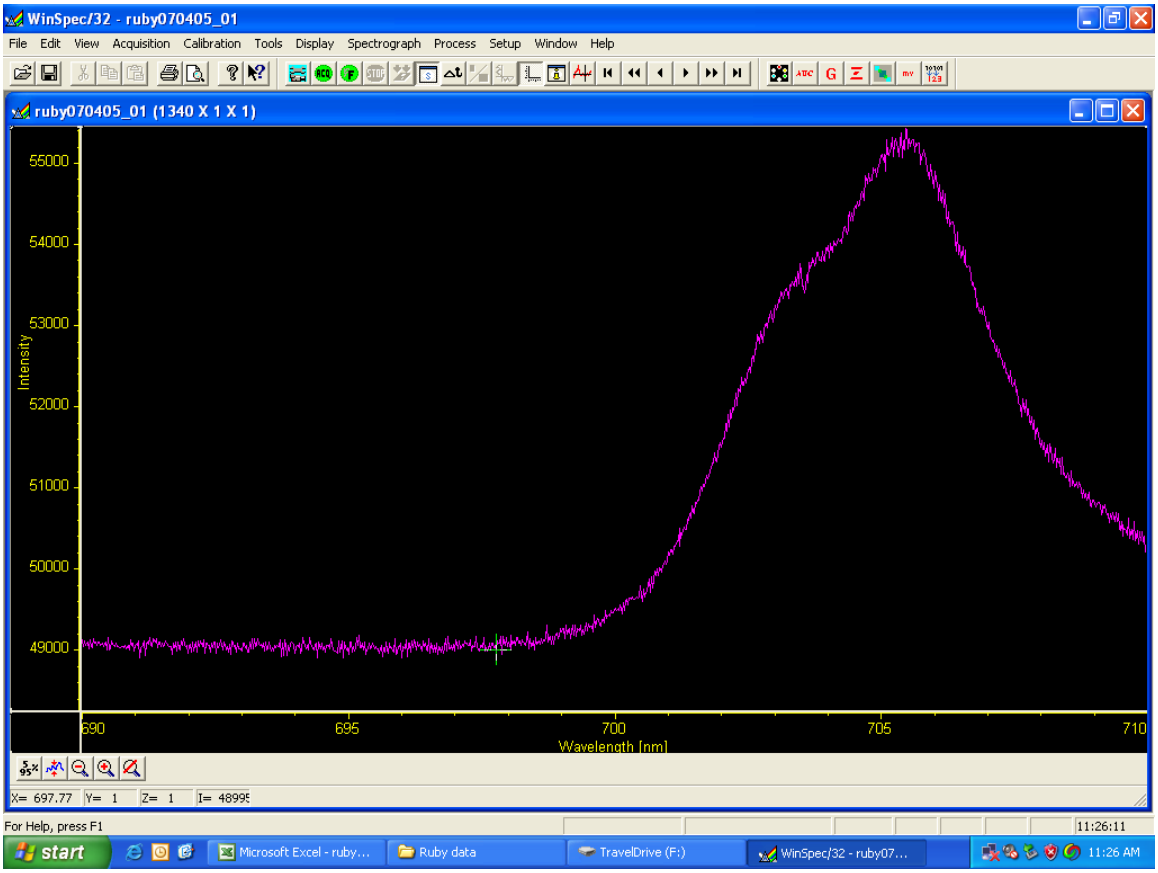

Figure 2. Ruby fluorescence spectrum at 30 GPa.

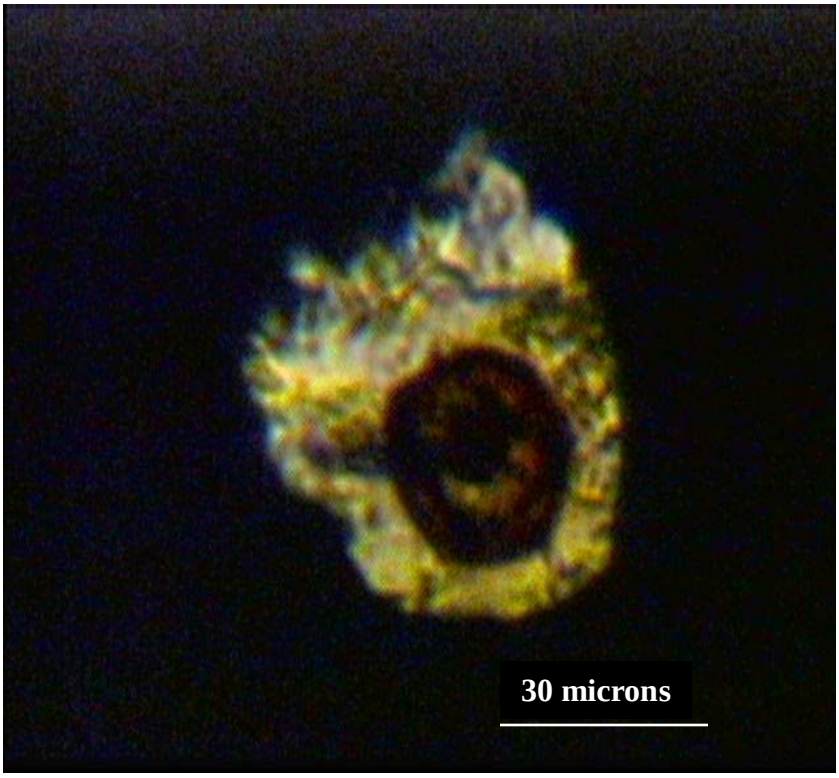

Figure 3. Illustrate a laser heated spot. From the rim to the core, there is a change in temperature gradient indicate melting, and change in composition.

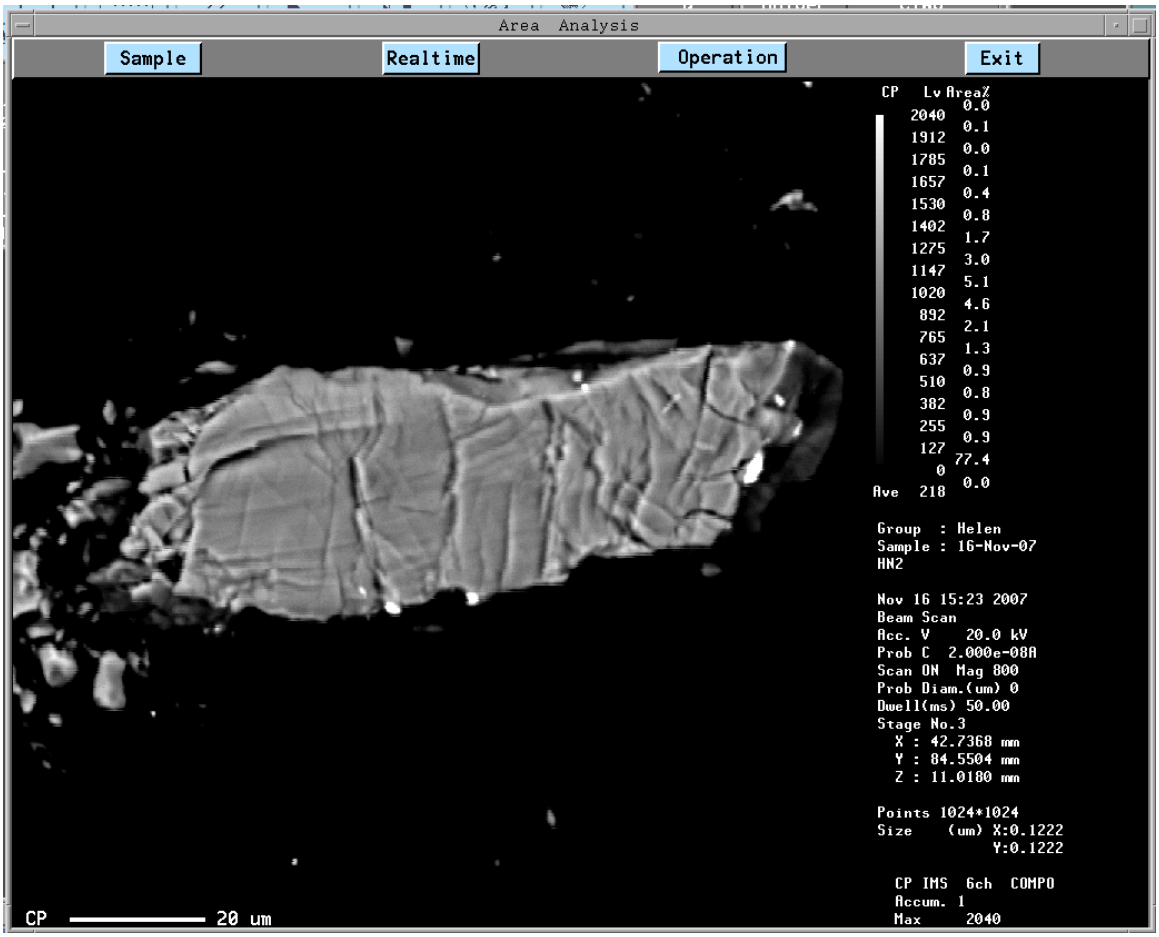

Figure 4 showed an SEM image that was taken from the EMP, we ran a 79.2 μm, 159 steps transect across the sample for and measured the composition, because of the temperature gradient, the melt is concentrated in the center, and the solid phase on the liquidus forms a ring around the melted spot.

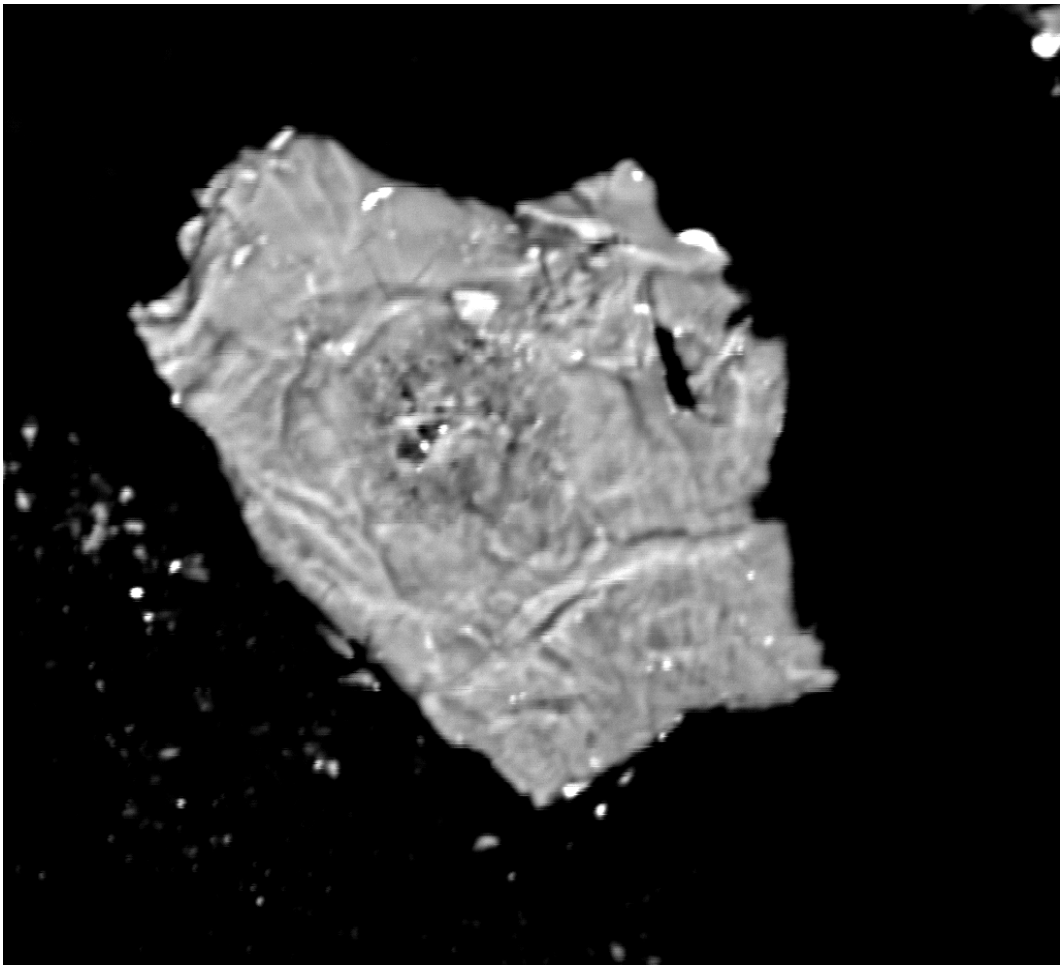

Figure 5 showed an SEM image that was taken from EMP when obtaining the EDS data, this experiment was at 40 GPa.

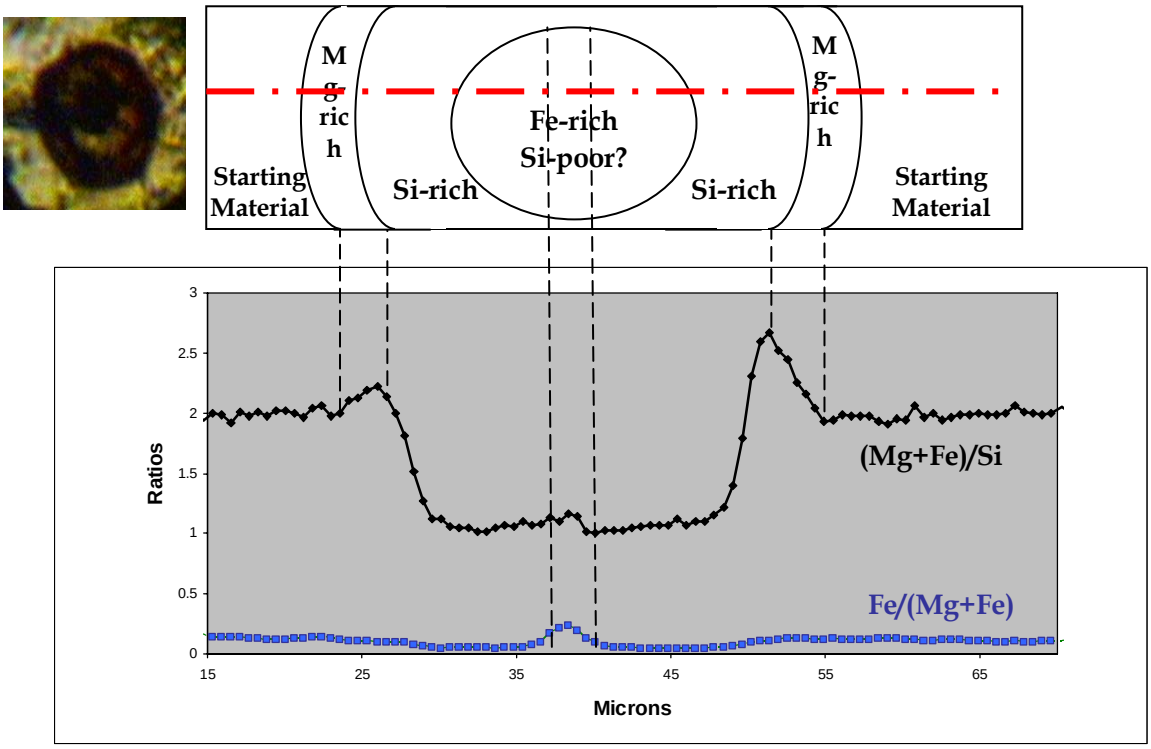

Figure 6 showed the EDS data that we obtain from the electron microprobe for experiment at 40 GPa. From the graph we have the starting material to begin with, as coming into the rim of the sample we found that is MgO rich, and Si-poor. As going into the lighter part where there is Soret diffusion causes the variation with the melted region, where we saw Si-rich, and in the center is Fe-rich. From the EDM data, it indicated that the phase on the liquidus at 40 GPa is magnesiowüstite, not silicate perovskite.

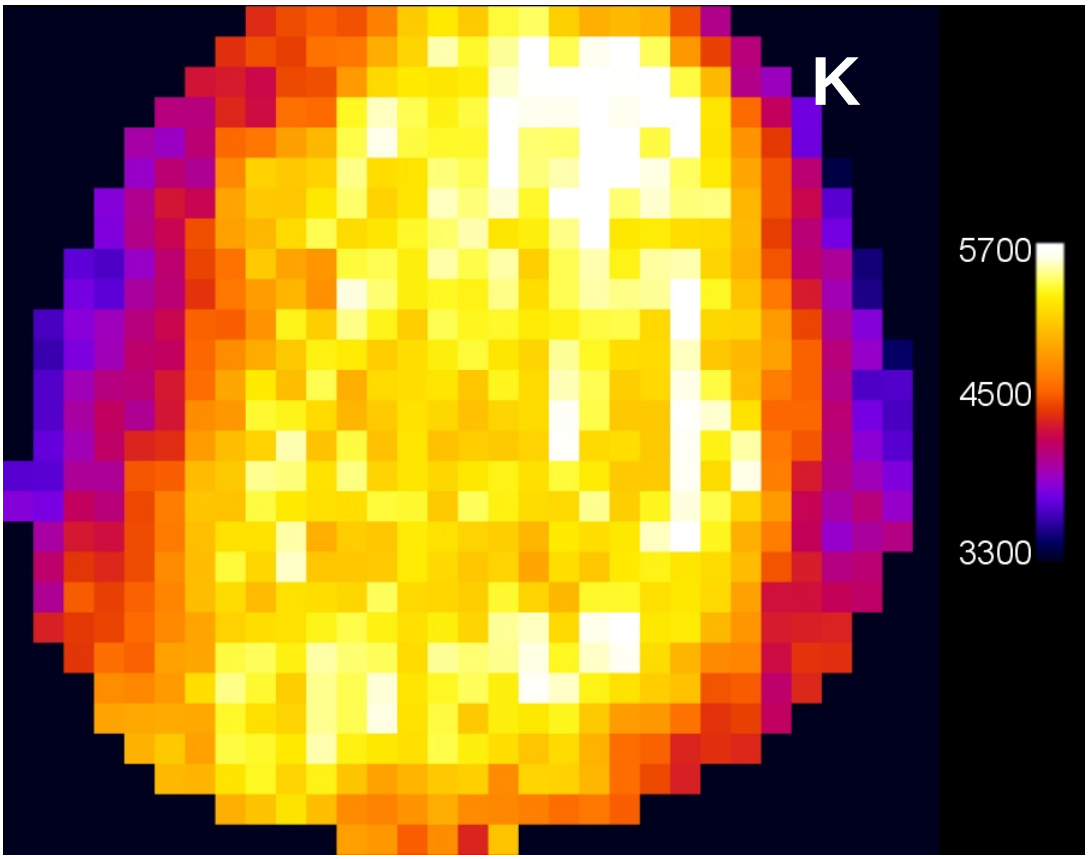

Figure 7 showed a 2D temperature map of a sample at 30 GPa, we found that the temperature is high above the published temperature of the pervoskite at the liquidus, we measured the temperature at 5240 K.

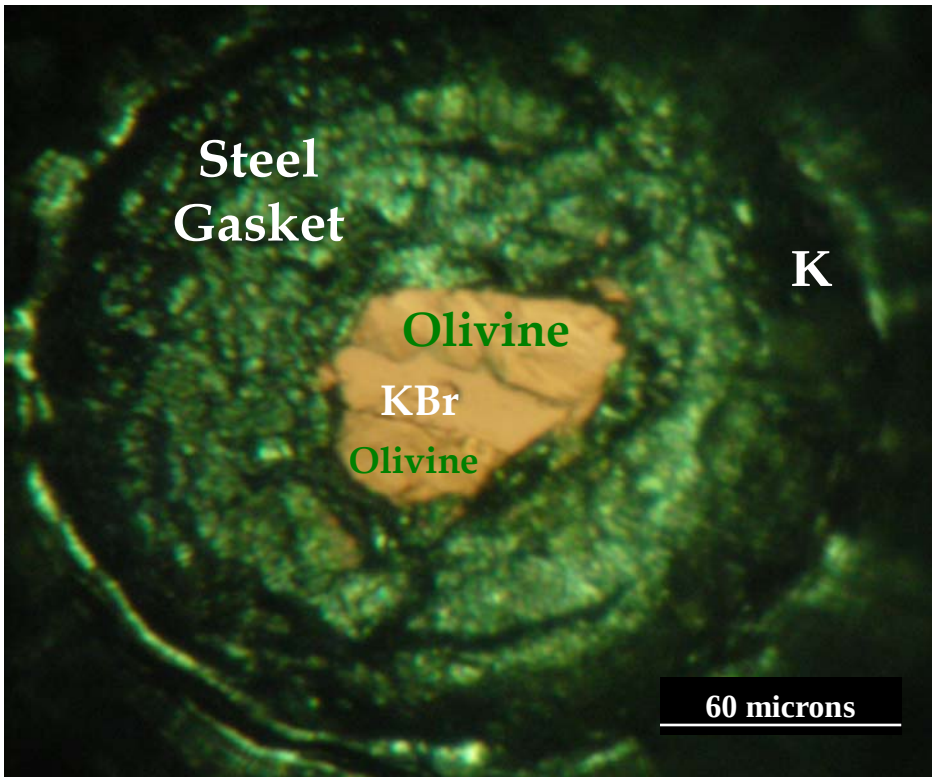

Figure 8a. Before laser heating

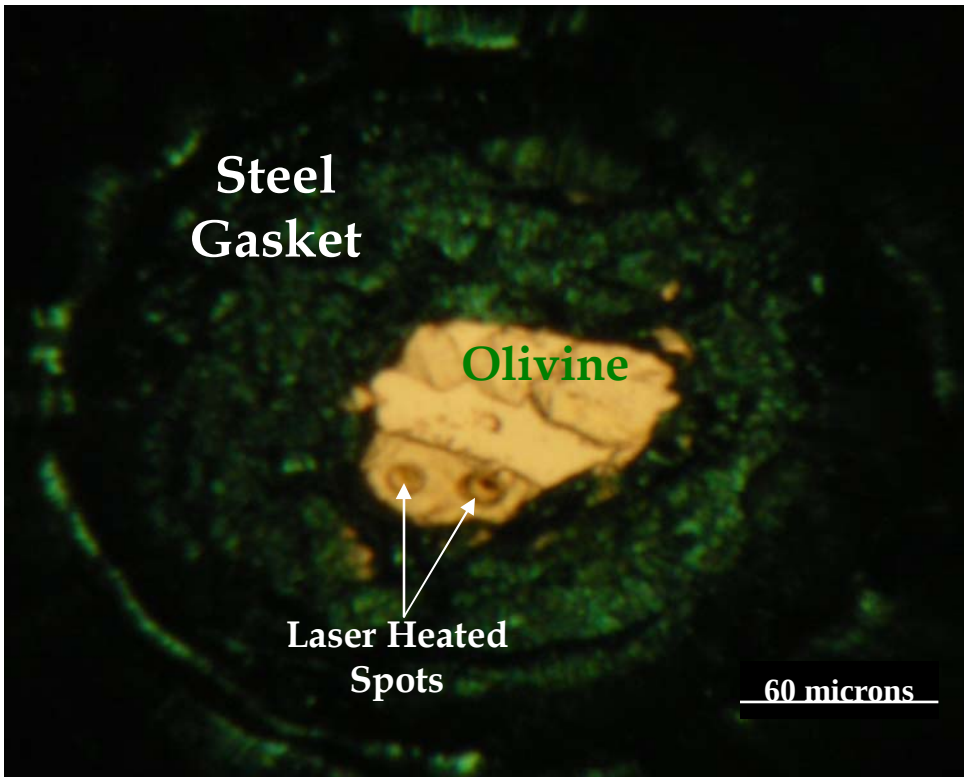

Figure 8b. After laser heating.

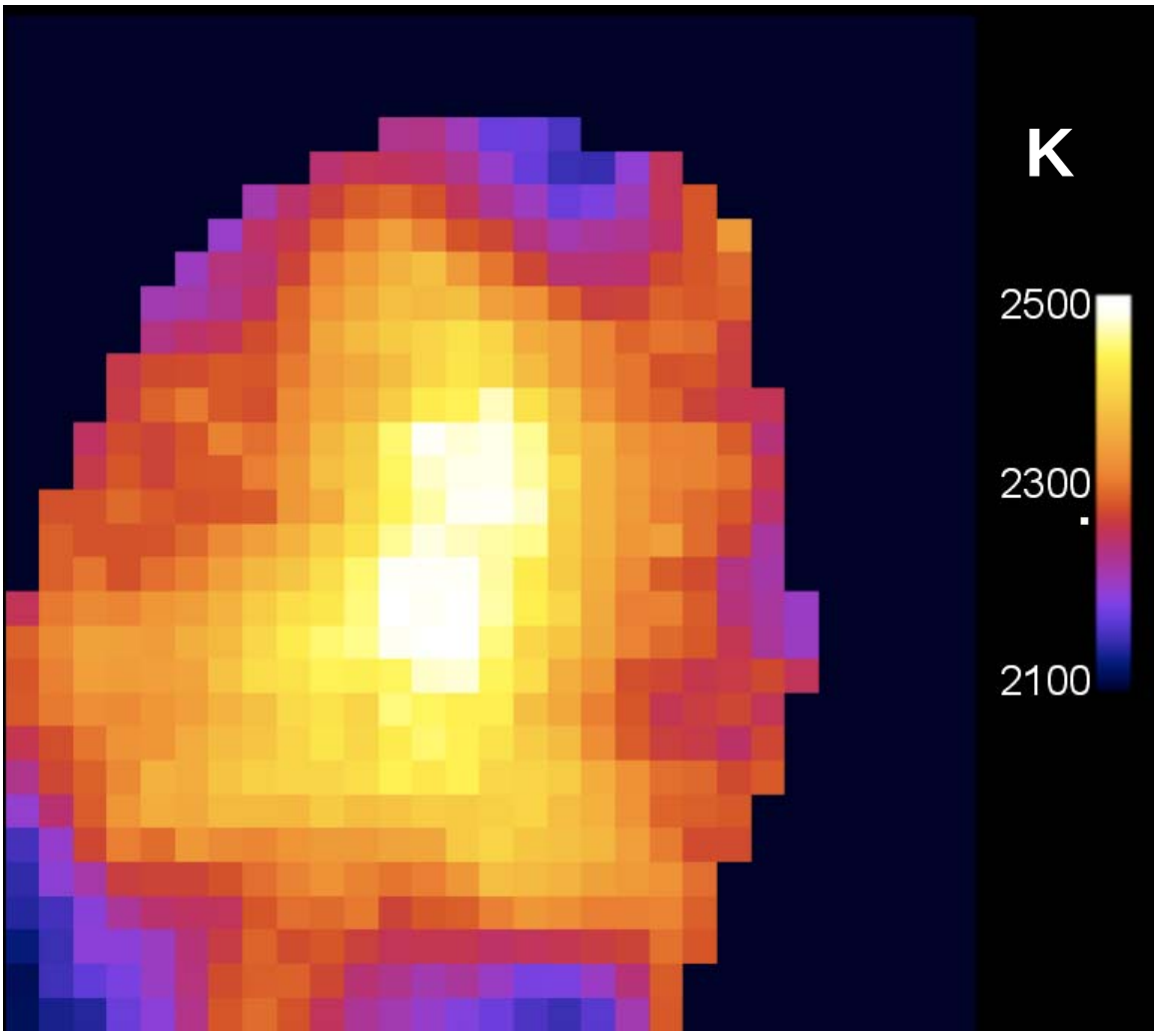

Figure 9 illustrated a 2D temperature map at 40 GPa, this temperature was more controllable because we changed the sample geometry, this sample was loaded with platinum foil.